ISBN: 978-3-95450-179-3 doi:10.18429/JACoW-FEL2017-WEP055

TAPERED FLYING RADIOFREQUENCY UNDULATOR*

S. V. Kuzikov†,2, A. V. Savilov, A. A. Vikharev
Institute of Applied Physics, Russian Academy of Sciences, Nizhny Novgorod, Russia
S. Antipov, A. Liu, Euclid Techlabs LLC, Bolingbrook, IL, USA
[2]Euclid Techlabs LLC, Bolingbrook, IL, USA

Abstract

We propose an efficient XFEL consisting of sequential RF undulator sections using: 1) tapered flying RF undulators, 2) short pulse, high peak-power RF and 3) driving undulator sections by spent electron beam. In a flying RF undulator, an electron bunch propagates through a high-power, nanosecond, co-propagating RF pulse. Helical waveguide corrugation supports a space harmonic with a negative propagation constant, providing a large Doppler up-shift. The undulator tapering technique improves FEL efficiency by 1-2 orders of magnitude in comparison with other facilities by decreasing the undulator period so that particles are trapped in the combined field of the incident x-ray and undulator field. We develop a so-called non-resonant trapping regime not requiring phase locking for feeding RF sources. Simulations show that by decreasing the corrugation periodicity one can vary an equivalent undulator period by 15%. The spent electron beam can be used to produce wakefields that will drive the RF undulator sections for interaction with the following beam. We have already manufactured and tested the 30-GHz simplified version of the 50-cm long undulator section for cold measurements and currently start low-power test of the tapered prototype.

FLYING-RF UNDULATOR

The RF undulator based on a travelling wave benefits from a Doppler up-shift when the electron beam interacts with oncoming microwaves. In [1] an RF pulse co-propagating (with the electron beam) was proposed where a benefit of the Doppler up-shift of Compton scattering is not lost due to the mode having strong -1st spatial harmonic transverse fields at axis of a helical corrugated waveguide (Figure 1). In this "flying" undulator the effective interaction length L_{eff} of a pulse with length τ and group velocity v_{gr} is proportional to $(1-v_{gr}/c)^{-1}$. For a large group velocity L_{eff} can be much larger than the pulse length.

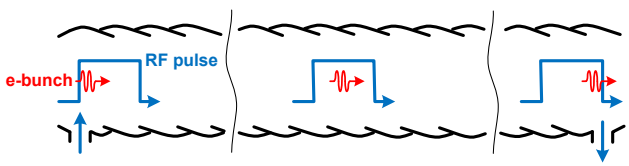

Figure 1: Flying RF undulator geometry (helical corrugation) and interaction timing structure.

*This work was supported by DoE Small Business Innovative Research Phase I Grant #DE-SC0017145.
†sergeykuzikov@gmail.com

In [1-2], a 30 GHz, 10 ns, 1 GW relativistic backward wave oscillator powers a 10-m long RF undulator with effective undulator strength $K = 0.3$ and undulator period $\lambda_u \approx 5$ mm. There are high power Ka-band BWO's which are good candidates for powering of the proposed flying undulator [3-4].

Figure 2 shows the dispersion characteristic of the operating mode of the TE_{11}-TM_{01}-TM_{11} RF undulator for the following geometrical parameters: $R_0 = 6.1$ mm, periodicity $D = 6$ mm and corrugation depth $a = 0.3$ mm (red solid curve). The dashed curve is the dispersion characteristic of the same mode in the waveguide with smaller corrugation period, 5.4 mm. Therefore, a tapered undulator can be built near 34 GHz using adiabatic variation of corrugation period so that the effective undulator period change is as high as 10%.

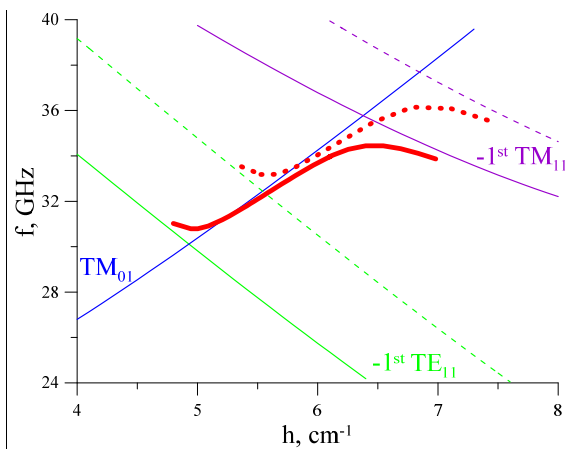

Figure 2: Dispersion of the operating mode (red solid curve) of the helical undulator with period of corrugation 6 mm and dispersion of this mode (red dashed curve) of the undulator with period of corrugation 5.4 mm.

HIGH-EFFICIENCY, TAPERED FLYING-RF UNDULATOR

For a high efficiency free electron laser we consider a string of tapered flying undulators (Figure 3). Each RF undulator section is assumed to be a helical corrugated structure with periodicity and corrugation depth changing as a function of z (coordinate along electron beam propagation).

ISBN: 978-3-95450-179-3 doi:10.18429/JACoW-FEL2017-WEP055

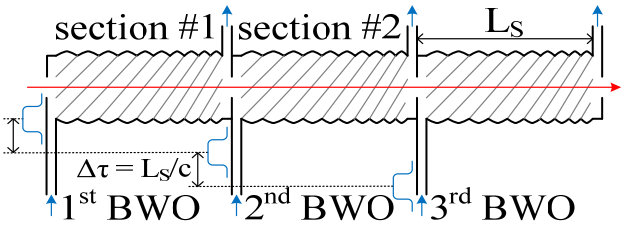

Figure 3: FEL scheme based on tapered RF undulators with decreasing equivalent undulator period.

In each undulator section geometrical parameters are varied to maintain the resonant condition ($\lambda \approx \lambda_u/2\gamma^2$) with particles losing their energy from γ_0 to γ_{min}, which defines the maximum efficiency $\eta = \Delta\gamma/(\gamma\text{-}1)$. The electron beam enters each undulator section at such time that it ends up in the tail of the RF pulse. As electrons travel along the undulator at virtually the speed of light they pass the RF pulse which has a group velocity slower than speed of light.

By the time the electron beam reaches the head of the RF pulse it has arrived at the exit of the undulator section. Electrons interact with both the RF field of the undulator and x-ray field generated by the electrons themselves. This interaction in a tapered undulator section can be represented in a phase space as a typical pendulum behavior with stationary buckets in which electrons are trapped (have finite trajectories). The center of the bucket corresponds to a resonant energy, and its size in energy is proportional to a current undulator parameter $K(z)$ as well as x-ray wave amplitude. Due to a finite signal rise and fall time electron beam sees initially a very small bucket due to low RF field. As it passes the RF pulse, at the exit of the undulator the bucket collapses again due to RF field roll off.

In the traditional resonant trapping scheme, considered for XFELs, electrons were assumed to be trapped in the bucket and stay in the same bucket the whole time, decreasing their energy from γ_0 to γ_{min}. For resonant trapping with RF undulators all undulator sections have to be at the same RF phase, meaning that all RF sources have to be phase locked. As it was proven in the experiment [4], phase locking of the mentioned BWOs is possible, but it dramatically increases cost of the XFEL.

We propose a so-called *non-resonant* trapping of electrons to relieve the stringent requirements on phase locking [5, 6]. In this scenario, not all electrons fall into the bucket at the entrance of the section. The ones that are trapped in a bucket stay trapped, and collapse inside the bucket, decreasing their energy due to radiation. The energy of other electrons does not change and they do not radiate. In the following sections another portion of electrons are trapped and decelerated. Going from section to section most of the electrons will end up decelerated.

Let us consider an example of XFEL calculations on a base of the described principles. In this example we take a 600 MeV ($\lambda \approx 2$ nm), 100 pC electron bunch of 0.167 ps length and 30 μm diameter. The energy spread is 0.1%. According to 1D FEL theory, Pierce parameter is as high as $\rho = 5\times10^{-4}$ (gain length $L_g \approx 0.5$ m). The FEL consists of 16 sections, each 10 m long, each section has sine-like tapering of the corrugation amplitude with undulator parameter $K_{max} = 0.25$ in maximum. In Figure 4, one can see variations of undulator period along the XFEL. The first two sections (first 20 m) with $\lambda_u = 5.5$ mm are necessary to excite initial x-ray wave which is to be amplified in next sections. All other sections are tapered ones. In these sections the magnitude of tapering increased along the distance. The further a given section from the entrance, the stronger it's tapering magnitude.

This law is necessary because in the beginning of the FEL the x-ray amplitude is rather small so that effective trapping of particles is not available. As the amplitude of the x-ray wave grows up the stronger tapering becomes possible which promises higher efficiency. In the considered example the last 16th section has 10% variation of the undulator period. The efficiency of the FEL was calculated using 1D theory equations. In Figure 5, the black curve (#1) corresponds to the simulation where all sections were phase locked. In this simulation, the highest efficiency (0.8%) was obtained.

Other simulations (curves #2-6) were performed with only the first two sections being phase locked and all other 14 sections had a uniform [0-2π] random distribution of RF phases from one section to another section. Note that calculated in these cases efficiencies are high, in the worst case (curve #4) the efficiency is approximately 15% less than in the best case (curve #1).

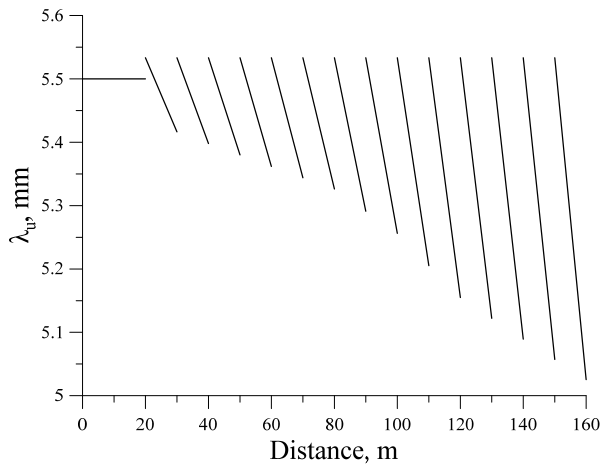

Figure 4: Dependence of effective undulator period in FEL consisted of individually tapered sections.

ISBN: 978-3-95450-179-3 doi:10.18429/JACoW-FEL2017-WEP055

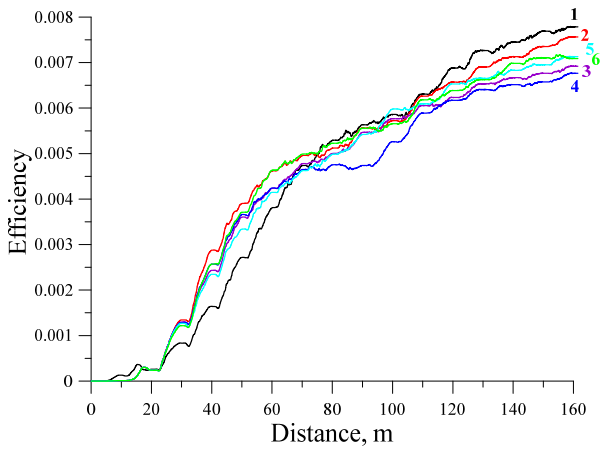

Figure 5: Efficiency of lasing along FELs for in-phase undulator sections (black curve#1) and for 5 different sets of sections with randomly distributed phases (curves 2-6).

Figure 6 represents particle distributions in the entrance of the simulated XFEL (blue dots) and in the exit (red dots). It is well seen that energies of most particles considerably reduced.

Note that the suggested principle of the non-resonant trapping allows further increase of the efficiency. The longer the XFEL, the higher efficiency could be reached. In the non-resonant trapping case, electrons that missed the bucket because of phase, frequency or amplitude drift are not lost completely as they have a chance to be trapped in the following section.

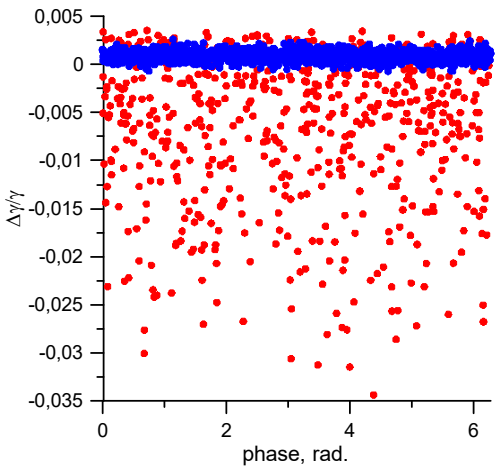

Figure 6: Energy-phase distribution of particles in the entrance of FEL (blue) and in its exit (red).

One more assertion follows from the calculations. According to Figure 6, the energy spread from section to section increased. Therefore, non-resonant trapping is well suitable for XFELs driven by bunches having large energy spread. In particular, bunches produced by means of laser-plasma acceleration technique can be used.

We are working to develop GENESIS simulation of lasing in the flying RF undulator.

LOW-POWER TEST

For low-power test we produced two prototypes of RF undulator sections made of aluminium using 3D printing technology. One is the described 20 cm long TE_{11}-TM_{01}-TM_{11} section with sine-like corrugation amplitude along section and 10% linear variation of undulator period (Figure 7). The second one is TE_{11}-TE_{21}-TM_{11} section with the same corrugation amplitude change law and 15% linear variation of the period (Figure 8).

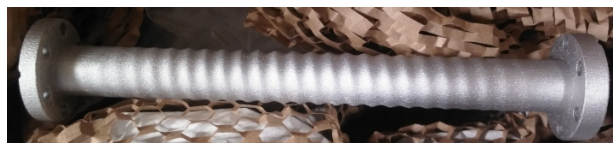

Figure 7: A 34 GHz TE_{11}-TM_{01}-TM_{11} RF undulator.

Figure 8: A 34-GHz TE_{11}-TE_{21}-TM_{11} RF undulator and a low-power experimental setup.

The low-power test is necessary to prove the desired tapering in a single RF undulator section. To obtain this goal we are going to use a scheme exploiting bead pull measurements of transverse fields along the longitudinal axis. In the mentioned undulator TE_{11}-TM_{21}-TM_{11} there are no any fields of 0^{th} harmonics at axis that is why, it is more convenient for measurements. For the test we first excite the rotating on azimuth TE_{21} mode by means of a mode converter consisted of two bends and a polarizer. Second, we feed the undulator by a standing wave produced by means of a Bragg reflector which reverses rotation of the TE_{21} mode (Figure 9). As a result, we can measure the standing wave field structure at axis and easily to compare undulator period in the beginning and in the end of the tested section correspondingly.

ISBN: 978-3-95450-179-3 doi:10.18429/JACoW-FEL2017-WEP055

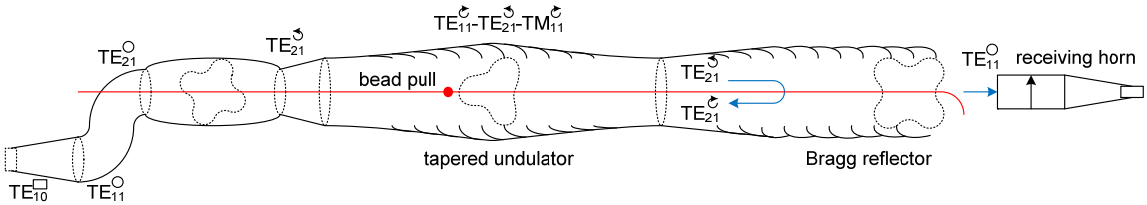

Figure 9: Scheme of low-power measurements.

CONCLUSION

Calculations show that high efficiency ~1% are achievable in a XFEL driven by 600 MeV bunches having 0.1% energy spread. The considered FEL consists of tapered undulator sections with varied waveguide period and operates basing on non-resonant trapping of particles. The proposed Ka-band RF undulators, fed by gigawatt level BWOs, allow keeping the mentioned efficiency of the XFEL even for non phase locked RF sources.

REFERENCES

[1] S. V. Kuzikov, A. V. Savilov, and A. A. Vikharev, "Flying radio frequency undulator", *Applied Physics Letters* 105, 033504 (2014). doi: 10.1063/1.4890586.

[2] E. B. Abubakirov *et al*., "Microwave undulators and electron generators for new-generation free-electron lasers", *Radiophysical Quantum Electronics* 58, p. 755 (2016). doi:10.1007 /s11141-016-9648-z.

[3] S. D. Korovin *et al*., "Generation of Cherenkov superradiance pulses with a peak power exceeding the power of the driving short electron beam", *Physical Review E* 74, 016501 (2006).

[4] V. V. Rostov, A. A. Elchaninov, I. V. Romanchenko, and M. I. Yalandin, "A coherent two-channel source of Cherenkov superradiance pulses", *Applied Physical Letters* 100, 224102 (2012).

[5] A. V. Savilov, "Cyclotron resonance maser with a tapered magnetic field in the regime of 'nonresonant' trapping of the electron beam", *Physical Review E* 64, p. 066501 (2001).

[6] A. V. Savilov, I. V. Bandurkin, N. Yu. Peskov, "Regime of non-resonant trapping in an FEM-amplifier", *Nuclear Instruments and Methods in Physics Research, Section A: Accelerators, Spectrometers, Detectors and Associated Equipment*, 507 (1-2), pp. 158-161 (2003).